JST: Smart Systems and Devices
Volume 34, Issue 1, January 2024, 051-057

Control of the Tower Crane Using Input Shaping-Sliding Mode Control

Minh Duc Duong, Minh Dung Le, Duy Long Le, Quy Thinh Dao*
Hanoi University of Science and Technology, Ha Noi, Vietnam
**Corresponding author email: thinh.daoquy@hust.edu.vn*

Abstract

Tower cranes are widely used for moving heavy goods, materials, or tools around a site. They help to speed up construction and save time and manpower in a process. However, a significant problem of tower cranes is oscillatory behavior, which can adversely impact safety and delivery accuracy. This paper proposes sliding mode control (SMC) combined with Input Shaping (IS) for controlling tower cranes. Sliding mode control itself can be used to control a tower crane to obtain position precision and vibration suppression. However, the selection of controller parameters may be difficult and the required control effort is high. In addition, chattering may occur. With the combination of input shaping, these problems can be overcome. The control parameter range is extended and the required control effort is reduced when input shaping is applied. In addition, input shaping also helps to reduce load vibration and chattering. Simulations in Matlab-Simulink have been done and the simulation results show the effectiveness of the proposed control algorithm.

Keywords: Tower crane, sliding mode control, input shaping, vibration suppression control.

1. Introduction

Tower crane control is difficult to do satisfactorily. It is challenging to obtain accurate positioning with little payload swing since tower cranes often operate in challenging situations (high altitude, severe interference, etc.). Tower crane systems, on the other hand, have extremely complex dynamics due to their high nonlinearity and significant state coupling. Tower cranes, in contrast to commonly used overhead cranes, also incorporate jib slew motion, which increases the likelihood that the cargo may swing in space and creates far more challenging control issues. Tower cranes' primary control responsibility is to precisely regulate the cargo to the appropriate position with swing suppression.

The tower crane is a flexible system's control may suffer as a result of modeling errors. To deal with the undesirable dynamic response resulting from both intentional motion and unexpected disturbances, several control systems have been developed. The capacity of sliding mode control to reject perturbations and pursue a planned trajectory has drawn a lot of interest. Methods for generating commands have gained popularity recently because of the way they can eliminate motion-induced vibration.

Sliding mode control is primarily used to reject disturbances and maintain insensitivity to parameter perturbations [1]. Even in the presence of parameter uncertainty, sliding mode control may deliver flawless trajectory tracking, according to [2]. Sliding mode control has been applied to control tower crane systems [3-6]. However, high actuator effort is the price to pay for flawless trajectory monitoring. The actuator is compelled to quickly change directions, which causes chatter, in order to maintain the system response along the required trajectory. The actuator's chattering may cause the system to experience certain high frequencies that weren't modeled. As the number of states rises, it becomes increasingly challenging to construct a sliding mode controller. It becomes even more challenging when these extra states are linked to ambiguous flexible modes.

Input shaping [7] is one type of command generation that has proven successful in many types of applications. Implementing input shaping involves convolving a desired system command with an impulse sequence known as the input shaper. The shaped input will not generate any residual vibration Many different systems have applied input shaping techniques for vibration suppression [8].

The combination of input shaping and other closed-loop control techniques has been considered in recent years to improve the system's performance. The combination of Input Shaping (IS) and Proportional - Derivative (PD) controllers has been implemented for overhead cranes to reduce the settling time in [9]. The combination of IS and Linear Quadratic Regulator (LQR) control is also studied in [10]. It is found that IS can improve the closed-loop system's performance.

From these combination suggestions, in this paper, the combination of IS and sliding mode control is proposed to control a tower crane. The sliding mode control first is applied to control the tower crane. Then, IS is used to improve the tower crane's performance.

ISSN: 2734-9373
https://doi.org/10.51316/jst.171.ssad.2024.34.1.7
Received: January 17, 2023; accepted: April 9, 2023

The rest of this paper is organized as follows: Section 2 introduces a dynamic model of a tower crane together with the SMC formulation. Experimental implementation and results are shown in Section 3. Finally, Section 4 concludes the contribution of the paper and the future works.

2. Modeling and Controller Design

2.1. Tower Crane Model

The coordinate definitions that are used in this thesis are shown in Fig. 1. The three concentrated masses in the crane system are the trolley mass m_t , the cargo mass m_c , and the equivalent rotating mass J of the tower. Correspondingly, three types of motion are determined, namely, translating motion of trolley x, rotating motion of tower γ, and sway motion of suspended cargo on cable characterized by swing angles φ and θ that describe how the load vibrates when the tower crane is in operation. To derive the tower crane's equations of motion, the Euler-Lagrange method is applied.

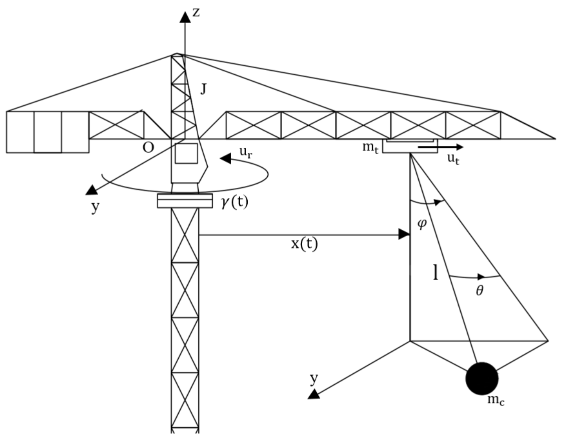

Fig. 1. Coordinate frames of a tower crane

The kinetic energy of the tower crane is determined by the sum of the kinetic energy of the load, the trolley, and the rotational kinetic energy of the tower body:

$$K = \frac{1}{2}m_t x_t^2 + \frac{1}{2}m_c x_c^2 + \frac{1}{2}J\dot{\gamma}^2 \tag{1}$$

The potential energy of the tower crane is:

$$P = -mgl\cos\theta\cos\varphi \tag{2}$$

The Lagrange function is determined according to the kinetic and potential energy expressions of the system:

$$L = K - P = \frac{1}{2}m_t x_t^2 + \frac{1}{2}m_c x_c^2 + \frac{1}{2}J\dot{\gamma}^2 + m_t l\cos\theta\cos\varphi \tag{3}$$

Since the internal load does not exert any force. The following is the given Lagrange's equation for the load-vibration motions:

$$\begin{cases} \dfrac{d}{dt}\left(\dfrac{\partial l}{\partial\dot{\theta}}\right) - \dfrac{\partial l}{\partial \theta} = 0 \\ \dfrac{d}{dt}\left(\dfrac{\partial l}{\partial\dot{\varphi}}\right) - \dfrac{\partial l}{\partial \varphi} = 0 \end{cases} \tag{4}$$

Assume the rotation angles are very small and ignore the change in cable length during the operation of the tower crane. For control design, the nonlinear components are ignored. Mathematical model of tower crane is obtained in matrix form as follows [11]:

$$\ddot{R} + \frac{m_c}{m_t}g\varphi = \frac{u_t}{m_t} \tag{5}$$

$$\left(1 + \frac{m_t}{J}R^2\right)\ddot{\gamma} - \frac{m_c}{J}gR\varphi = \frac{u_r}{m_t} \tag{6}$$

$$l\,\ddot{\theta} + g\theta + R\,\ddot{\gamma} = 0 \tag{7}$$

$$l\,\ddot{\varphi} + g\varphi + \ddot{R} = 0 \tag{8}$$

2.2. Sliding Mode Control

Position regulation and anti-swing control are the two objectives of the proposed control strategy. As a result, we create a controller that pushes the girder, trolley, and load into the desired positions. Additionally, by acting as an anti-swing control, the designed controller forces the φ and θ components of the swing angle to zero.

The sliding mode controller's purpose is to drive actuated to reach desired values and cargo swing angles to approach zero. Assume that all state variables are quantifiable. First, a first-order sliding surface is defined to draw all state trajectories, and then a control scheme is built to force all system states to their reference values on the sliding surface.

To facilitate the controller design process, it is necessary to set the following variables:

$$x_1 = R; \quad x_3 = \gamma; \quad x_5 = \phi; \quad x_7 = \theta$$

$$\dot{x}_1 = x_2; \quad \dot{x}_3 = x_4; \quad \dot{x}_5 = x_6; \quad \dot{x}_7 = x_8$$

Then the mathematical equation of the model will include the following equations:

$$\begin{aligned} \dot{x}_1 &= x_2 \\ \dot{x}_2 &= \frac{u_t}{m_t} + \frac{m_c}{m_t}gx_5 \\ \dot{x}_3 &= x_4 \\ \dot{x}_4 &= \frac{u_r J}{m_t(J + m_t x_1^2)} + \frac{mgx_1x_7}{J + m_t x_1^2} \\ \dot{x}_5 &= x_6 \\ \dot{x}_6 &= \frac{\dot{x}_2}{l} - \frac{gx_5}{l} \\ \dot{x}_7 &= x_8 \\ \dot{x}_8 &= -x_1\frac{\dot{x}_4}{l} - \frac{gx_7}{l} \end{aligned} \tag{9}$$

To satisfy the trolley control and the angle of rotation of the tower crane shaft to the desired position, set the values for the position to $x_{1d} = R_d$, for the angle to be $x_{3d} = \gamma_d$.

Define the following regulation error vectors, as follows:

$$\begin{aligned} e_1 &= x_{1d} - x_1 \\ e_3 &= x_{3d} - x_3 \\ e_5 &= -x_5 \\ e_7 &= -x_7 \end{aligned} \tag{10}$$

Define the positive defined matrices μ_1, μ_2 and α such that

$$\mu_1 = \begin{bmatrix} \mu_{11} & 0 \\ 0 & \mu_{12} \end{bmatrix};\ \mu_2 = \begin{bmatrix} \mu_{21} & 0 \\ 0 & \mu_{22} \end{bmatrix};\ \alpha = \begin{bmatrix} \alpha_1 & 0 \\ 0 & \alpha_2 \end{bmatrix}$$

Choose the following sliding surface:

$$s_1 = \dot{e_1} + \mu_{11} e_1 + \alpha_1 \dot{e_5} + \mu_{21} e_5 \tag{11}$$

$$s_2 = \dot{e_3} + \mu_{12} e_3 + \alpha_2 \dot{e_7} + \mu_{22} e_7 \tag{12}$$

The task of control design is to determine the control signal u_t, u_r to move the system towards the sliding surface and keep it on it.

We will denote the control signal u_t, u_r as follows:

$$u_t = \begin{cases} u_{teq} \text{ when } s_1(x,t) = 0 \\ u_{tN} \text{ when } s_1(x,t) \neq 0 \end{cases} \tag{13}$$

$$u_r = \begin{cases} u_{req} \text{ when } s_2(x,t) = 0 \\ u_{rN} \text{ when } s_2(x,t) \neq 0 \end{cases} \tag{14}$$

where u_{ieq} is the signal component that keeps *x(t)* on the slide (equivalence principle), u_{iN} is the component that causes the signal *x(t)* to move towards the slip surface (*i = t, r)*. Differentiating the sliding surface with respect to time, one can obtain:

$$\dot{s_1} = \ddot{e_1} + \mu_{11} \dot{e_1} + \alpha_1 \ddot{e_5} + \mu_{21} \dot{e_5} \tag{15}$$

$$\dot{s_2} = \ddot{e_3} + \mu_{12} \dot{e_3} + \alpha_2 \ddot{e_7} + \mu_{22} \dot{e_7} \tag{16}$$

By setting $\dot{s_1} = 0$ and $\dot{s_1} = 0$ we obtain the following results.

$$u_{teq} = \frac{m_t l}{\alpha_1 + l}\Big(\ddot{x}_{1d} + \dot{x}_{1d} - \mu_{11} x_2 + \frac{\alpha_1 g}{l} x_5 - \mu_{21} x_6\Big) - m_c g x_5 \tag{17}$$

$$u_{req} = \frac{(J + m_t x_1^2) l m_t}{J(l - \alpha_2 x_1)}\Big(\ddot{x}_{3d} + \mu_{12} \dot{x}_{3d} - \mu_{12} x_4 + \frac{\alpha_2 g}{l} x_7\Big) - \frac{m_t m g}{J} x_1 x_7 \tag{18}$$

To control the system to move towards the sliding surface, the control signal is chosen as:

$$u_{tN} = -K_1 sign(s_1) \tag{19}$$

$$u_{rN} = -K_2 sign(s_2) \tag{20}$$

Therefore, the overall SMC scheme composed of approximated control and switching action is written by:

$$u_t = \frac{m_t l}{\alpha_1 + l}\Big(\ddot{x}_{1d} + \dot{x}_{1d} - \mu_{11} x_2 + \frac{\alpha_1 g}{l} x_5 - \mu_{21} x_6\Big) - m_c g x_5 - K_1 sign(s_1) \tag{21}$$

$$u_r = \frac{(J + m_t x_1^2) l m_t}{J(l - \alpha_2 x_1)}\Big(\ddot{x}_{3d} + \mu_{12} \dot{x}_{3d} - \mu_{12} x_4 + \frac{\alpha_2 g}{l} x_7\Big) - \frac{m_t m g}{J} x_1 x_7 - K_2 sign(s_2) \tag{22}$$

Controller coefficients $K_1, K_2, \mu_1, \mu_2, \alpha$ are selected so that the sliding surface is stable, and the state trajectories slide to desired values on surface as quickly as possible.

2.3. Stability Analysis

Two requirements must be met by the SMC scheme: (1) Control scheme forces state trajectories to reach sliding surface (reaching condition); and (2) After entering the sliding surface, the control scheme pulls state trajectories there to the desired values (sufficient condition).

To analyze stability condition of the system, one can consider a Lyapunov candidate function:

$$V = V_1 + V_2 = \frac{1}{2} s_1^2 + \frac{1}{2} s_2^2 \geq 0 \tag{23}$$

where $V_1 = \frac{1}{2} s_1^2$ and $V_2 = \frac{1}{2} s_2^2$

Then:

$$\dot{V_1} = s_1 \dot{s_1} \tag{24}$$

$$\dot{V_2} = s_2 \dot{s_2} \tag{25}$$

Substitute (11)-(22) into (24) and (25) we get:

$$\dot{V_1} = -K_1 \frac{\alpha_1 + l}{m_t l} s_1 sign(s_1) = -c_1 |s_1|; \tag{26}$$

$$\dot{V_2} = -K_2 \frac{J(l - \alpha_2 x_1)}{l m_t (J + m_t x_1^2)} s_2 sign(s_2) = -c_2 |s_2| \tag{27}$$

where $c_1 = K_1 \frac{\alpha_1 + l}{m_t l}$ and $c_2 = K_2 \frac{J(l - \alpha_2 x_1)}{l m_t (J + m_t x_1^2)}$.

It is easy to see that $\dot{V_1} \leq 0$ for all positive define K_1, K_2, α_1. In order to obtain $\dot{V_2} \leq 0$, the following condition must hold:

$$l - \alpha_2 x_1 > 0 \tag{28}$$

Since x_1 is the translation of the trolley, it is bound, i.e., $x_1 \leq M_m$. By choosing $\alpha_2 < \frac{l}{M_m}$, the condition (28) is held. Thus, $\dot{V} = \dot{V_1} + \dot{V_2} \leq 0$, the system is stable at $s_1 = 0$ and $s_2 = 0$.

In addition,

$$(|s_1| + |s_2|)^2 = s_1^2 + s_2^2 + 2|s_1||s_2| \geq s_1^2 + s_2^2 \tag{29}$$

Thus,

$$\begin{aligned} \dot{V} = \dot{V}_1 + \dot{V}_2 &= -c_1|s_1| - c_2|s_2| \\ &\leq -c(|s_1| + |s_2|) \\ &\leq -c(s_1^2 + s_2^2)^{\frac{1}{2}} \\ &= -cV^{1/2} \end{aligned} \tag{30}$$

where $c = \min(c_1, c_2) > 0$.

According to [12], the function $V(t)$, $s_1(t)$ and $s_2(t)$ converge to zero in a finite time. In addition according to [4], $s_1 = 0$ and $s_2 = 0$ can lead to $e_1 = 0, e_3 = 0, e_5 = 0, e_7 = 0$, i.e., the system is stable at $R = R_d, \gamma = \gamma_d, \varphi = 0, \theta = 0$.

2.4. Simulations of the Sliding Mode Controller

To verify the effectiveness of the sliding mode controllers, the simulation is done with the following conditions. In the first case, the trolley is controlled to translate 2 [m]. In the second case, the tower is driven to rotate to 0.7 [rad] (a desired angle) in the first 20 seconds and continuously to rotate to 0.5 rad (reference) in the next 30 seconds.

Table 1. Simulation parameter

Parameters	Value
g	9.81 [m/s^2]
l	3 [m]
m_t	50 [kg]
m_c	5 [kg]
J_0	30 [kg.m^2]

The value of the input control signal of the system shown in Fig. 2, includes two signals, pulling force and rotation torque. It can be seen that the two input control values are quite large.

Fig. 3 shows the response of the system following the shaped trajectory. The blue solid line is the reference value, and the red dashed curve is the output trajectory using the controller. Although there is fluctuation, it is not significant, follows quite closely to the initial set value, the system is relatively stable.

Fig. 4 shows the oscillation angle. Both oscillation angles, are relatively small oscillations and the oscillation suppression time does not take too long.

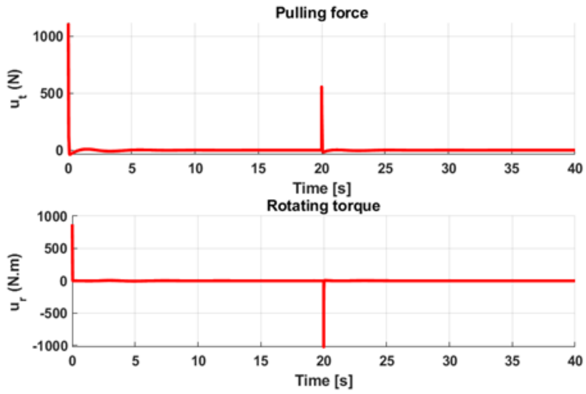

Fig. 2. The input control signal value (SMC)

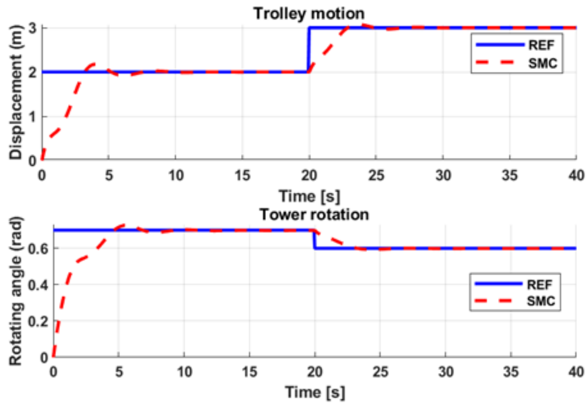

Fig. 3. System response (SMC)

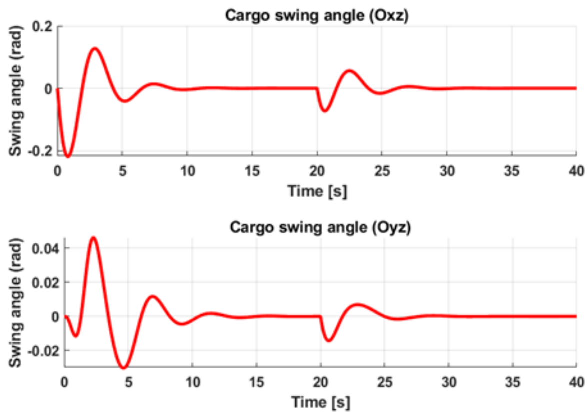

Fig. 4. Cargo swing angle (SMC)

Realize that with although the controller has stability, the input control signal is relatively large. Thus, we proceed to change the parameters to reduce the control input. Set $\mu = \mu_{min} = (0.2; -9; 0.2; 1)$, the control input in this case is shown in Fig. 5, and the system response in two cases $\mu = \mu_{max}$ and $\mu = \mu_{min}$ are compared in Fig. 6 and Fig. 7. When μ is reduced, the system already has a control signal significantly smaller than a larger value of μ.

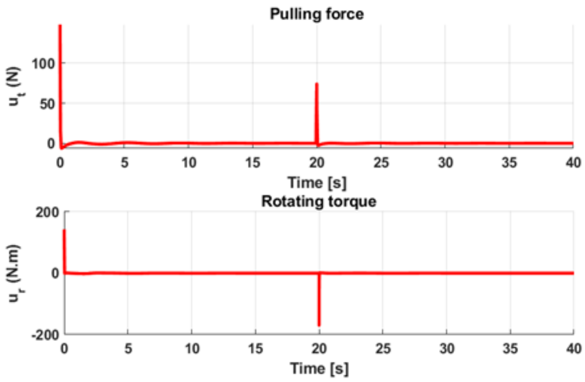

Fig. 5. The input control signal value (SMC)

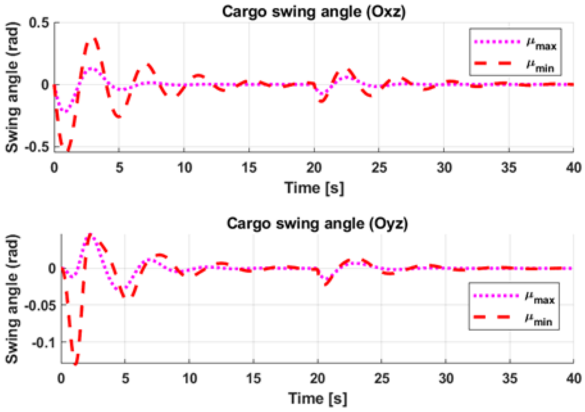

Fig. 7. Cargo swing angle (SMC)

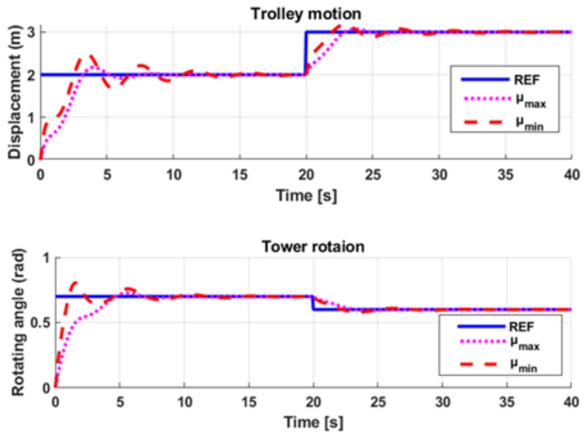

Fig. 6. System response (SMC)

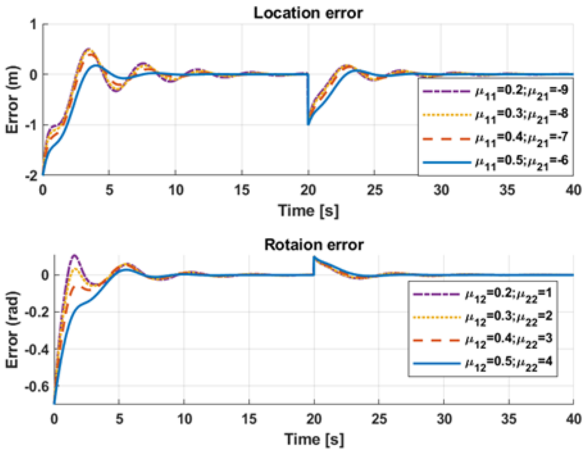

Fig. 8. Tracking Error (SMC)

Although tracking to the reference value, there are still fluctuations, especially in the rotation angle component. In addition, the response time is also relatively slow. Similar to the response of the system, the two oscillation angles of the system both fluctuate largerly. The time for the system to stop oscillation is relatively long. The moving trajectory of the load fluctuates quite a bit, especially when approaching the second set point.

Fig. 8 shows the decrease in the error corresponding to the higher values of μ. The higher the value of μ, the lower the error, indicating that the higher the μ-factor, the better the controller responds. To address the drawbacks identified in both of the aforementioned cases, an improvement can be made by incorporating Input Shaping into the controller.

3. Input Shaping and Input Shaping-Sliding Mode Controller.

In order to minimize oscillations and enhance the performance of the controller, including response time, stability, trajectories, and oscillation angles, it is proposed to integrate an Input Shaping into the existing controller.

3.1. Input Shaping Technique

A vibratory system can be considered as a second order underdamped system of the form:

$$G(s) = \frac{\omega_n^2}{s^2 + 2\xi\omega_n s + \omega_n^2} \tag{31}$$

where ω_n is the natural frequency and ξ is the damping ratio of the system in the time domain. The response of the system with amplitude A_i at time $t_i$can be expressed as

$$y(t) = A_i \frac{\omega_n}{\sqrt{1-\xi^2}} e^{-\xi\omega_n(t-t_i)} \times \sin\left(\omega_n \sqrt{1-\xi^2}(t-t_i)\right) \tag{32}$$

To suppress the vibration of an impulse, a series of impulses is input to the system. The amplitude and time of these impulses are determined by setting the total system response after the last impulse equal to zero. From this, the following results are obtained. For the case of 2 impulses, it is Zero Vibration (ZV) the impulse parameters are as follows:

$$\begin{bmatrix} t_i \\ A_i \end{bmatrix} = \begin{bmatrix} 0 & \frac{\pi}{\omega_d} \\ \frac{K}{1+K} & \frac{1}{1+K} \end{bmatrix} \quad (33)$$

$$K = e^{\frac{\xi\pi}{\sqrt{1-\xi^2}}}$$

For the case of 3 impulses, it is Zero Vibration Derivative (ZVD), the impulse parameters are as follows:

$$\begin{bmatrix} t_i \\ A_i \end{bmatrix} = \begin{bmatrix} 0 & \frac{\pi}{\omega_d} & \frac{2\pi}{\omega_d} \\ \frac{K^2}{(1+K)^2} & \frac{2K}{(1+K)^2} & \frac{1}{(1+K)^2} \end{bmatrix} \quad (34)$$

$$K = e^{\frac{\xi\pi}{\sqrt{1-\xi^2}}}$$

3.2. Input Shaping-Sliding Mode Control for Tower Crane

To combine input shaper and sliding mode control, the tower crane is controlled by a sliding mode controller as in Section 2. In addition, the input shaper is added as feedforward controller to the system. The input shaper plays a role in shaping the reference trajectory before it is put into the system with sliding mode controller.

The input shaping with 2 impulses is considered in this paper. In order to calculate the input shaper, the natural frequency of the tower crane model is chosen. With $\omega_n = \sqrt{g/l} = 1.81$ (rad/s), $\xi = 0$ we can calculate the amplitude and time of the input pulses:

$$K = e^{\frac{\xi\pi}{\sqrt{1-\xi^2}}} = 1; \Delta T = \frac{\pi}{\omega_n} = 1.74 \text{ (s)} \quad (35)$$

$$A_1 = \frac{K}{1+K} = \frac{1}{2}, t_1 = 0$$

$$A_2 = \frac{K}{1+K} = \frac{1}{2}, t_2 = \Delta T$$

With the same simulation parameters as in Section 2, we get the results as shown in figures from Fig. 9 to Fig. 12. The value of the input control signal of the system shown in Fig. 9, includes two signals, pulling force and rotation torque. Both values are equivalent to the value of SMC which is not too large.

Fig. 10 shows the response of the system following the shaped trajectory. The system is more stable, both the angle and position values of the trolley are closer to the set value, the oscillations have been significantly reduced compared to using SMC controller alone.

Fig. 11 shows that the oscillation angle was significantly reduced when adding IS to the sliding mode controller. The value can be considered as relatively small and the oscillation time is also short, thereby determining that the IS-SMC is more stable during migration.

Fig. 12 shows the decrease in the error corresponding to the higher values of μ. The error for the IS-SMC system is significantly smaller than the error for the system using the SMC with the same value of μ.

It is found that when adding IS, the oscillation is significantly reduced compared to using conventional SMC and gives an equivalent position. This means that the proposed control algorithm can reduce the chattering phenomenon, in comparison to the conventional SMC controller. The reason is the proposed controller can accept the higher value of μ that reduces the chattering effect.

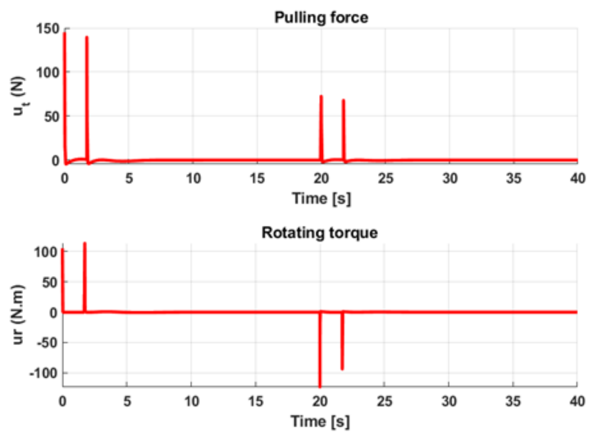

Fig. 9. The input control signal value (IS-SMC)

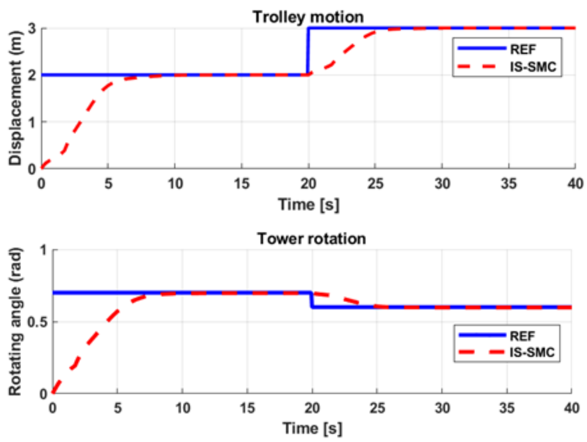

Fig. 10. System response (IS-SMC)

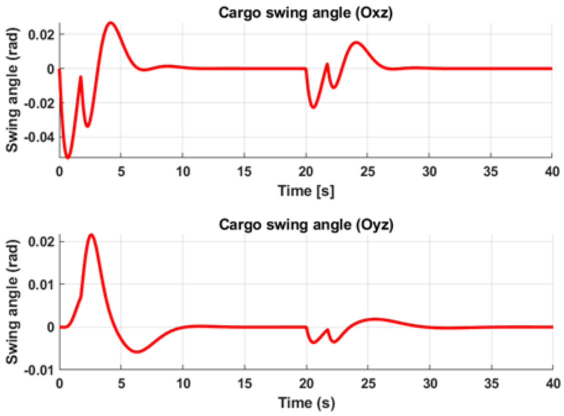

Fig. 11. Cargo swing angle (IS-SMC)

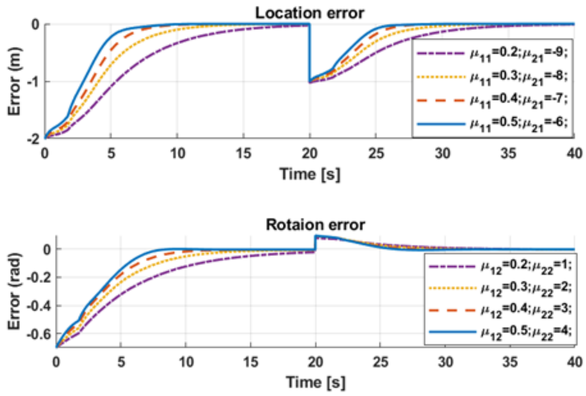

Fig. 12. Tracking Error (IS-SMC)

4. Conclusion

In this paper, it has been demonstrated that a tower crane system's tracking performance can be improved by a control strategy that combines an input shaping and a sliding mode controller. Compared to the same system following an unshaped path, the overall error for the system following the shaped path is significantly lower. An increase in the system's rise time is the cost of enhancing tracking performance. The increase in rise time, however, might not be noticeable if the system's rise time is very brief in comparison to the entire maneuver length. The kind of shaper being used directly affects how long the rise time takes to increase. Based on the simulation results, the application of the IS-SMC practical model demonstrates promising outcomes, providing favorable and stable results. Furthermore, the integration of IS into the SMC system leads to a reduced adverse effect on the load during operation.

In the future, the proposed control algorithm will undergo practical implementation to validate its effectiveness. Furthermore, there is also consideration for extending the control algorithm to include tower crane systems with varying rope lengths. This expansion aims to address the specific challenges associated with such systems and further enhance the control capabilities.

References

[1] Young, K.D., V. I. Utkin, and U. Ozguner, A control engineer's guide to sliding mode control. IEEE Transactions on Control Systems Technology, 1999. https://doi.org/10.1109/87.761053

[2] Slotine, J. J. and W. Li, Applied Nonlinear Control, Englewood Cliffs, NJ: Prentice-Hall, Inc., 1991.

[3] Vázquez C., Fridman L, Collado J., and Ismael Castill, Second-order sliding mode control of a perturbed-crane. Journal of Dynamic Systems, Measurement, and Control 137, no. 8, 2015. https://doi.org/10.1115/1.4030253

[4] Qian D., Yi J., Hierarchical Sliding Mode Control for Under-actuated Cranes. Heidelberg, Berlin: Springer, 2016 https://doi.org/10.1007/978-3-662-48417-3

[5] Le T. A., Dang V-H, Ko D. H., An T. N., Lee S-G. Nonlinear controls of a rotating tower crane in conjunction with trolley motion. Proceedings of the Institution of Mechanical Engineers, Part I: Journal of Systems and Control Engineering, 227(5):451-460, 2013. https://doi.org/10.1177/0959651812472437

[6] Aboserre L. T., El-Badawy A. A. Robust integral sliding mode control of tower cranes. Journal of Vibration and Control, 27(9-10):1171-1183, 2021. https://doi.org/10.1177/1077546320938183

[7] Singer, N. C. and W. P. Seering, Preshaping command inputs to reduce system vibration. J. of Dynamic Sys., Measurement, and Control, 112, pp. 76-82, 1990. https://doi.org/10.1115/1.2894142

[8] Singhose, W. Command shaping for flexible systems: A review of the first 50 years. Int. J. Precis. Eng. Manuf. 10, 153-168, 2009. https://doi.org/10.1007/s12541-009-0084-2

[9] M. D. Duong, Q. T. Dao, and T. H. Do, Settling time optimization of a critically damped system with input shaping for vibration suppression control, Eng. Technol. Appl. Sci. Res., vol. 12, no. 5, pp. 9388-9394, Oct. 2022. https://doi.org/10.48084/etasr.5242

[10] Muenchhof, Marco, and Tarunraj Singh, Concurrent feed-forward/feedback design for flexible structures, In AIAA Guidance, Navigation, and Control Conference and Exhibit, p. 4941, 2002. https://doi.org/10.2514/6.2002-4941

[11] Hanafy M. Omar, Control of gantry and tower cranes, PhD thesis, Virginia Polytechnic Institute and State University, January 2003.

[12] S. Mobayen, Adaptive global terminal sliding mode control scheme with improved dynamic surface for uncertain nonlinear systems, International Journal of Control, Automation and Systems, vol. 16, no. 4, pp. 1692-1700, 2018 https://doi.org/10.1007/s12555-017-0473-8